Tehran International Congress on Manufacturing Engineering (TICME2005)
December 12-15, 2005, Tehran, Iran

Achieve to desired weld bead geometry for the vessel fillet joints in mobile robotic welding

M. Golestani Sehat[1], Kh. Farhangdoost[2]
Mechanical Engineering Department
Ferdowsi University, mashhad, Iran;
Corresponding Author E-mail:
m.golestan@gmail.com

Abstract
Employing of the mobile robot manipulators for fillet joint welding of vessel is presented in this paper. Have desired weld bead geometry for fillet joints is the objective of this work. The welding process variables which influence weld bead shape, are coupled with each other but not directly connected with weld bead shape individually. The relationships between welding process parameters and weld bead geometry are very difficult and complicated. The task is to track the horizontal fillet seem in the vessel, while the weld bead shape - criteria for quality of weldment - is desired. Here, using of optimum design based on mathematical model to obtain welding process parameters that necessary to programming of mobile robot manipulators. The system discussed in this paper is the nonholonomic mobile manipulators built from a robotic arm mounted on a wheeled mobile platform. We use of the manipulability considerations to generate the controls of our system to track seem by end effector. Simulation results were also presented to demonstrate the capability of this system to provide of our requirement.

Keywords*:* Mathematical Model, Fillet Welding, Mobile Manipulators, Manipulability, Nonholonomy

1 Introduction
Weld bead geometry is influenced by a large number of welding process parameters. The relationships between GMAW process parameters and weld bead geometry are very complex and difficult because of the number of parameters involved and nonlinear relationships. The mathematical model is one approach to show these relationships [1-3]. Welding process parameters such as welding current, arc voltage, welding speed, gas flow rate and offset distance are highly coupled, thus making it difficult to derive a mathematical relationship between them. It is necessary to selection of the appropriate welding process parameters for the desired weld bead shape in the adequate boundary conditions. Optimum design [4,5], which is based on mathematical model, was successfully applied to the welding processes for selecting the optimal welding parameters for the desired weld bead shape.

[1] - M.Sc Student, Mech. Eng. Dept. Ferdowsi University
[2] - Assistant professor, Mech. Eng. Dept. Ferdowsi University

To make effective use of automated and robotic arc welding, it is imperative that a mathematical model which can be programmed easily and fed to the robot should be developed. It should provide a high degree of confidence in predicting the weld bead geometry and shape relations to accomplish the desired mechanical properties of the weldment. The mathematical model should also cover a wide range of material thicknesses and be applicable for all welding positions. For the automatic welding system, the data must be available in the form of mathematical equations.
Kim and Kwon [1], obtained a mathematical model for weld bead geometry of partial-penetration, single-pass, bead-on-plates in GMAW. also Kim and Son [2], used of mathematical model that explained relationships between bead penetration for robotic CO_2 arc welding.
Mobile manipulators built from a wheeled mobile platform and a robotic arm. Thus, these systems combine manipulation and mobility capabilities. The arrangement of the wheels and their actuator determine the holonomic or nonholonomic nature of these locomotion systems.
The objective of this paper is welding of horizontal fillet joints in vessel by mobile manipulator, while the weld bead shape is desired. So we use five measures for weld shape, and obtain five welding process parameter by optimum design for different thickness of vessel plate [4].

2 Experimental process

For study the relationships between the weld bead shape and welding process parameters, need to a definition for weld shape. fillet joint shapes are define by five measure, such as leg length1, leg length2, penetration, throat thickness and reinforcement height, as shown in Figure 1. In this paper we used of Hyeong-Soon Moon and Suck-Joo Na'reserch [4]. For welding the fillet joint, the welding process variables included welding current, arc voltage, welding speed, gas flow rate and offset distance. All other parameters except these were fixed Solid wire AWS

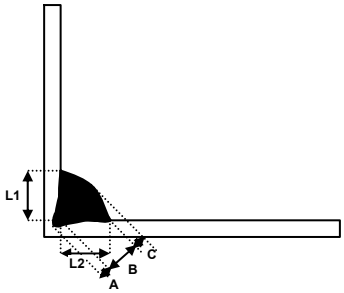

L1: Leg length 1
L2: Leg length 2
A: penetration
B: Throat thickness
C: Reinforcement height

Figure1: A schematic diagram for weld bead shape

ER70s-6 of 1.2 mm diameter were used. The shielding gas composition was Ar (80%) and CO_2 (20%). Here focused on the vessels that assembled from plate with different thickness. To explanation the relationships between welding parameters and weld bead shape need to set of experimental data. The ranges of welding parameters for three thickness of plate were used are shown in table 1. Hyeong-Soon Moon and Suck-Joo Na[4] were performed 20 experiment for each thickness of base metal. Usage of these results is in the mathematical models.

Table 1
Welding variables and limits employed

Thickness of Base metal (mm)	Range of weld parameters (Min-Max)				
	Welding Speed (mm/s)	Arc Voltage (V)	Welding Current (A)	Gas Flow Rate (L/min)	Offset Distance (mm)
4.5	4-8	20-26	200-260	14-18	0-2
6	4-8	23-29	220-300	14-18	0-2
7	4-8	26-31	250-350	14-18	0-2

3 Development of mathematical models

In order to quantitatively evaluate the effect of welding process parameters on the fillet weld bead shape, the mathematical model for relationship between process parameters and weld bead shape have been developed. In general, the response function can be represented as follows:

$$y = f(x_1, x_2, x_3, x_4, x_5, x_6) \quad (1)$$

Where y is a variable indicating the weld bead shape (mm), x_1 is the thickness of the vessel base metal (mm), x_2 is the welding speed (mm/s), x_3 is the arc voltage (V), x_4 is the welding current (A), x_5 is the gas flow rate (L/min) and x_6 is the offset distance (mm).

Because the relationship between welding variables and weld bead shape is nonlinear, Eq.(1) can be expressed as follows:

$$y = (x_1^{\,a} x_2^{\,b} x_3^{\,c} x_4^{\,d} x_5^{\,e} x_6^{\,f}) \quad (2)$$

Where the empirical coefficients a, b, c, d, e and f are constants. The values a, b, c, d, e and f were computed by the method of nonlinear multiple regression. These analyses were carried out with the help of a standard statistical package (SAS). Based on the regression analysis using the least square method from experimental results, the following equations can be estimated [4]:

$$y_1 = x_1^{0.095} x_2^{-0.520} x_3^{0.152} x_4^{0.557} x_5^{-0.367} x_6^{0.0036} \quad (3)$$

$$y_2 = x_1^{0.266} x_2^{-0.583} x_3^{0.473} x_4^{0.338} x_5^{-0.331} x_6^{0.010} \quad (4)$$

$$y_3 = x_1^{0.484} x_2^{-0.003} x_3^{-0.517} x_4^{0.540} x_5^{-0.595} x_6^{0.006} \quad (5)$$

$$y_4 = x_1^{0.192} x_2^{-0.517} x_3^{-0.565} x_4^{0.089} x_5^{-0.099} x_6^{0.005} \quad (6)$$

$$y_5 = x_1^{0.259} x_2^{-0.227} x_3^{-2.652} x_4^{1.546} x_5^{0.104} x_6^{0.005} \quad (7)$$

Where y_1 is the leg length1 (mm), y_2 is the leg length2 (mm), y_3 is the penetration (mm), y_4 is the throat thickness (mm) and y_5 is the reinforcement height (mm).

4 Optimization

In welding of the vessel fillet joints, the optimal welding process parameters for achieve the desired weld bead shape are necessary. One of the important problems to be solved in the vessel welding process is to develop the mathematical model for the determination of optimum welding process parameters [5]. Unlike analytical model, that it is limitations such as its need for many assumptions to formulate the

equations and the complexity of the welding processes, experimental models such as nonlinear regression are capable to exactly predict the welding process.
In this paper the formulations of the optimization problem with five welding process variables and five variables indicating the welding surface profile for different thickness of the vessel base metal were

$$\begin{aligned} &for\,any\ x_1 \quad by\,changing \quad x_2, x_3, x_4, x_5, x_6 \\ &\min mize\ f(y_1, y_2, y_3, y_4, y_5) = (y_{d_1} - y_1)^2 + (y_{d_2} - y_2)^2 + (y_{d_3} - y_3)^2 + (y_{d_4} - y_4)^2 + (y_{d_5} - y_5)^2 \\ &Subjected\ \ to \\ &x_{2,\min} \le x_2 \le x_{2,\max}, x_{3,\min} \le x_3 \le x_{3,\max}, x_{4,\min} \le x_4 \le x_{4,\max}, x_{5,\min} \le x_5 \le x_{5,\max}, x_{6,\min} \le x_6 \le x_{6,\max} \end{aligned} \qquad (8)$$

Where the quadratic program was used to determine the appropriate welding conditions. y_i are the variables indicating the welding surface profile and computed from Eqs.(3)-(7), while y_{d_i} are the desired values of y_i.
An optimization spreadsheet was created based on the EXCELL™ solver to find the maximum welding speed for all combinations of parameters using the formulation in Equation (8). For some desired vessel weld bead shape, the optimal welding parameters that obtained from solver spreadsheet are shown in Table 2.

5 Modelling of the mobile manipulator

A mobile manipulator is a wheeled mobile platform with a multilink manipulator mounted on it as shown in Figure2.The wheeled mobile platform has two independent driving wheels which are at the center of each side and two passive castor wheels which are at the center of the front and the rear of the platform [6]. The manipulator has three revolute joints, and it moves in horizontal plane. If we leave out of account the angular value at the wheels, to define the platform configuration is equivalent to define the configuration of a rectangle on a plane. Its generalized coordinates are then three in number: two for position and one for the orientation. Let $\mathbf{q_p} = [x \quad y \quad \phi]^T$,

Table 2
The result of optimization procedure for some desired weld bead shape

Thickness of Vessel base metal (mm)	Desired variables indicating the Welding surface profile (mm)					Optimal welding process variables				
	y_{d_1}	y_{d_2}	y_{d_3}	y_{d_4}	y_{d_5}	x_2	x_3	x_4	x_5	x_6
4.5	4 5 5.5	4.5 6 5.5	1.5 1.3 1.6	3.5 4.5 4	1 2 1.4	8 5.4 5.4	23 20 21	200 200 220	18 18 14	0 0 0
6	5 6 5.7	5 6.5 4.7	1.9 2.5 1.9	3.6 4.7 4	1.3 1 1.5	7.4 8 6.9	23 27 23	220 291 220	14 14 14	0 2 0
7 *	7 8 5.3	7 9 6.5	1.3 2 1.8	5 5.7 4.2	1 1.5 1.2	4.6 4 6.8	26 26 26.5	250 264 250	16 14 18	0 0 2

y_{d_1}=leg length1, y_{d_2}=leg length2, y_{d_3}=penetration, y_{d_4}=throat thickness, y_{d_5}=reinforcement, x_2=welding speed, x_3=arc voltage, x_4=welding current, x_5=gas flow rate, x_6=offset distance

where x and y are the abscissa and the ordinate of the middle point of the driven wheels axle and ϕ is the angle made by the axis of symmetry and the vector $\vec{\mathbf{x}}$.

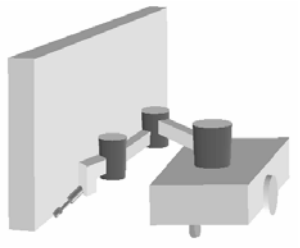

Figure 2: mobile manipulator with three-link

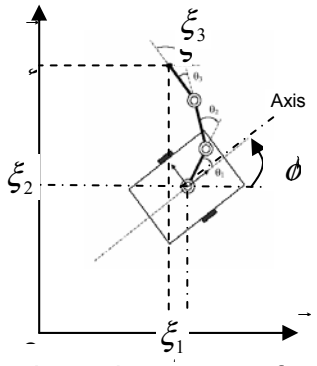

Figure 3: schematic diagram of mobile manipulator

For the mobile manipulator, the generalized coordinates are followed (see Figure 3):

$$\mathbf{q} = [x \quad y \quad \phi \quad \theta_1 \quad \theta_2 \quad \theta_3]^T \tag{9}$$

The location of the end effector is defined by position of end effector and orientation of the terminal link relative to vector $\vec{\mathbf{x}}$ and can be see in Fig. 3. Its location can be defined by three coordinates:

$$\xi = [\xi_1 \quad \xi_2 \quad \xi_3]^T \tag{10}$$

5.1 Nonholonomic constraint

The nonholonomic constraint for the mobile platform is that the platform must move in the direction of the axis of symmetry, i.e.,

$$\dot{x}\sin\phi - \dot{y}\cos\phi = 0 \tag{11}$$

This relation expresses the dependency between $\dot{x}$ and $\dot{y}$. Thus there are two independent admissible generalized velocities for the platform [6]. These two independent parameters can be shown by mobility control vector $\eta_P = [v \quad \omega]^T$ where, v is the velocity of the middle point of the driven wheels axle along its path and $\omega = \dot{\phi}$.

5.2 The direct kinematics of the MM

In the kinematics we consider the relation between the manipulator configuration and end effector location. Direct kinematics expresses the end effector location as a function of the manipulator configuration. The direct kinematic equations of the mobile manipulator are obtained as follows:

$$\xi_1 = x_c + l_1 c_{\phi 1} + l_2 c_{\phi 12} + l_3 c_{\phi 123} \quad \xi_2 = y_c + l_1 s_{\phi 1} + l_2 s_{\phi 12} + l_3 s_{\phi 123} \quad \xi_3 = \phi + \theta_1 + \theta_2 + \theta_3 \tag{12}$$

Where

$$s_{\phi 1} = \sin(\phi + \theta_1), c_{\phi 1} = \cos(\phi + \theta_1), s_{\phi 12} = \sin(\phi + \theta_1 + \theta_2), c_{\phi 12} = \cos(\phi + \theta_1 + \theta_2)$$

$$s_{\upsilon 123} = \sin(\upsilon + \theta_1 + \theta_2 + \theta_3), \; c_{\upsilon 123} = \cos(\upsilon + \theta_1 + \theta_2 + \theta_3)$$

5.3 The velocity kinematics of the MM

The mobile manipulator jacobian matrix, $J(q)$, transforms velocities in joint space to velocities of the end effector. This relation is shown as follows:

$$\dot{\xi} = J(q)\dot{q} \tag{13}$$

That the jacobian matrix is given as follows:

$$J(q)=\begin{bmatrix}1 & 0 & D_1 & D_2 & D_3 & D_4\\ 0 & 1 & D_5 & D_6 & D_7 & D_8\\ 0 & 0 & 1 & 1 & 1 & 1\end{bmatrix}$$

with:

$$D_1=-(l_1s_{\phi 1}+l_2s_{\phi 12}+l_3s_{\phi 123}), D_2=-(l_1s_{\phi 1}+l_2s_{\phi 12}+l_3s_{\phi 123}), D_3=-(l_2s_{\phi 12}+l_3s_{\phi 123}), D_4=-l_3s_{\phi 123}$$

$$D_5=l_1c_{\phi 1}+l_2c_{\phi 12}+l_3c_{\phi 123}, D_6=l_1c_{\phi 1}+l_2c_{\phi 12}+l_3c_{\phi 123}, D_7=l_2c_{\phi 12}+l_3c_{\phi 123}, D_8=l_3c_{\phi 123}$$

The mobility control vector for whole mobile manipulator is given as following [6]:

$$\eta=[\eta_P^{\ T}\quad \dot{\theta}_i^{\ T}] \tag{14}$$

The relation that expresses the dependency between η and $\dot{q}$ is in form:

$$\dot{q}=S(q)\eta \tag{15}$$

Therefore, we can be express $\dot{\xi}$ in term of η by following relation:

$$\dot{\xi}=\bar{J}(q)\eta \tag{16}$$

Where

$$S(q)=\begin{bmatrix}c_\upsilon & 0 & 0 & 0 & 0\\ s_\upsilon & 0 & 0 & 0 & 0\\ 0 & 1 & 0 & 0 & 0\\ 0 & 0 & 1 & 0 & 0\\ 0 & 0 & 0 & 1 & 0\\ 0 & 0 & 0 & 0 & 1\end{bmatrix} \quad \text{and} \quad \bar{J}(q)=\begin{bmatrix}c_\phi & D_1 & D_2 & D_3 & D_4\\ s_\phi & D_5 & D_6 & D_7 & D_8\\ 0 & 1 & 1 & 1 & 1\end{bmatrix}$$

5.4 The inverse velocity kinematics of the MM

In the inverse velocity kinematics, the joints velocity, $\dot{q}$, can be obtained from the end effector velocity in operational space. For achieve to this relation, it is necessary to computation of reduced inverse velocity kinematics [6] to obtain η. Then, using of relation (15) to computation $\dot{q}$. The reduced inverse velocity kinematics writes as:

$$\eta=\bar{J}^{+}(q)\dot{\xi}+(I-\bar{J}^{+}(q)\bar{J}(q))z(t) \tag{17}$$

Where $\bar{J}^{+}(q)$ is an arbitrary generalized inverse of $\bar{J}(q)$,such as the pseudo-inverse or Moore-penrose-inverse. And $z(t)$ is an arbitrary column matrix.

The mobile manipulator is track the seem by end effector with the operational error $e(t)$. Thus:

$$\begin{aligned} e&=\xi^d-\xi\\ \dot{e}&=\dot{\xi}^d-\dot{\xi}\end{aligned} \tag{18}$$

Where ξ^d and $\dot{\xi}^d$ are desired location and velocity of end effector respectively. To control of this transient error, use of following equation:

$$\dot{e}+\lambda e=0 \tag{19}$$

Where λ is the matrix that including the proportional gains. Thus:

$$\dot{\xi}=\dot{\xi}^d+\lambda(\xi^d-\xi) \tag{20}$$

By substitution of Eq.(20) in Eq.(17), we have:

$$\eta = \bar{J}^{+}(q)(\dot{\xi}^{d} + \lambda(\xi^{d} - \xi) + (I - \bar{J}^{+}(q)\bar{J}(q))z(t) \quad (21)$$

In this equation the first term is due to the input and the second one is the internal motion. We get $z(t)$ as follows:

$$z(t) = -k((\nabla^{T} P)H)^{T} \quad (22)$$

Where k is positive scaler and $H = S(I - \bar{J}^{+}\bar{J})$. Then by substitution of Eq.(22) in Eq.(21), the mobility control vector is:

$$\eta = \bar{J}^{+}(q)(\dot{\xi}^{d} + \lambda(\xi^{d} - \xi) - kS^{T}HH^{T}\nabla P \quad (23)$$

Where ∇P is gradient of manipulability measure, P, that were discussed in next section.

5.5 The manipulability of MM

The manipulability is the ability to move and apply forces in arbitrary directions (Park and Kim, 1998). Whereas (Bicchi and Prattichizza, 2000) define it as "the directions in the task space that extermize the ratio between some measure of effort in the joint space and a measure of performance in task space". Here we focus only on using kinematic manipulability in evaluating the welding mobile manipulator performance in various relative configurations [7-10].

Different algebraic measures have been proposed to the manipulability. One of these measures is Yoshikawa's measure of manipulability (Yoshikawa, 1985) and shown as follows:

$$P = \sqrt{\det(\bar{J}\bar{J}^{T})} \quad (24)$$

The other manipulability measure, extending the notation of eccentricity of the ellipse (Bayle et al., 2001):

$$P = \sqrt{(1 - \frac{\sigma_{k}^{2}}{\sigma_{1}^{2}})} \quad (25)$$

Where σ_{i} is the singular value of the jacobian matrix. In this paper, the Jacobian matrix that we used to obtain the Singular Values (Using Singular Value Decomposition), is the Jacobian of the whole mobile Manipulator: mobile platform and arm. Thus, the Manipulability Measure is for the MM. Beside this, we also separate the Manipulability Measure of the Arm (P_{arm}) and also the Manipulability Measure of the entire MM ($P_{arm+platform}$) using the following Equation:

$$P = \varepsilon P_{arm+platform} + (1 - \varepsilon)P_{arm} \quad (26)$$

Where ε is a weighting value and $P_{arm+platform}$ computed by using of $\bar{J}(q)$ and Eq. (24) or Eq. (25). Otherwise, P_{arm} computed by using of Eq. (24) or Eq. (25) and $J_{arm}(q)$ can be expressed as:

$$J_{arm} = \begin{bmatrix} C_{1} & C_{2} & C_{3} \\ C_{4} & C_{5} & C_{6} \end{bmatrix}$$

With:

$$C_1 = -l_1 s_1 - l_2 s_{12} - l_3 s_{123}, C_2 = -l_2 s_{12} - l_3 s_{123}, C_3 = -l_3 s_{123}$$
$$C_4 = l_1 c_1 + l_2 c_{12} + l_3 c_{123}, C_5 = l_2 c_{12} + l_3 c_{123}, C_6 = l_3 c_{123}$$

Finally, by using of Eq. (26) for P in MM and numerically calculation of ∇P, mobility control vector or η can be obtained from Eq. (23)

6 Path planning for welding of fillet joint in vessel

Robotic welding operations require trajectory control of the welding torch mounted on the end effector of the mobile manipulator, which is defined by the weld seem. The problem is positioning a welding torch with the proper location with respect to a given weld seem.

The schematic of mobile manipulator for welding of cubic and cylindrical tanks are shown in Figure 4. The mobile manipulator must be move in floor of the tank to track seem by the welding torch mounted on its end effector.

In this paper, the considered fillet joint were made with a torch work angle of γ and a torch travel angle of μ push. Where γ can be adjust by mounted torch on the end effector of mobile manipulator, while for maintenance of the welding torch in angle μ, it is necessary to adjustment of ξ_3. Thus, for each dimension of the tank, we can be programming of the welding mobile manipulator to track the seem by end effector with take into account of desired weld bead shape and γ and μ angles.

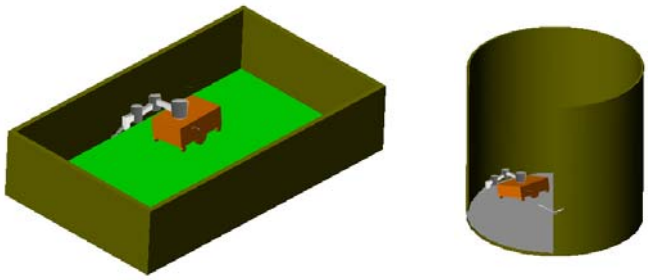

Figure 4: welding of vessel fillet joints by MM

7 Simulations and results

In this section, some simulation results are presented to demonstrated the effectiveness of the considered algorithm developed for horizontal fillet welding in the vessels. Here, we were focused on cubic tank and used of MATLAB code for simulations. Table 3 shows the kinematic parameters for the welding mobile manipulator and vessel used in this simulation. The condition of weld bead shape that used in simulation is shown in Table 2 by $*$.

Table 3
Numerical values of kinematic parameters of MM and vessel for simulation

parameter	values	parameter	values
Length of platform	0.6 m	Length of link 3	0.2 m
Width of platform	0.4 m	Length of tank	4.25 m
Length of link 1	0.4 m	Width of tank	2.83 m
Length of link 2	0.4 m		

We were used of Eq. (23) to simulation of welding mobile manipulator. In this equation, it is necessary to numerical calculation of ∇P. Where used from Eqs. (24)

or (25) to calculation P. The mobile manipulator must be move in floor of the tank and track seem by torch that mounted on its end effector. the planer position of rectangular seem of cubic floor, that used in this simulation is shown in Figure 6. It is important that the welding torch moves at a constant speed and maintains a constant inclination angle of $(\pi/2-\mu)$ in the plane to the weld seem. In this figure can be see the manipulability trapezoid for arm only and whole mobile manipulator that specified by blue and red colour respectively.

We were taken a $\mu=15^{\circ}$ in this simulation. For this value, the magnitude of ξ_3 must be equal to $-\pi/6$ for the first side of rectangular seem (a, in Figure 5) and $\pi/3$ for the second side of the rectangular seem (b, in Figure 5). Figure 6 shows the magnitudes of ξ_3 for the welding mobile manipulator in the primal section of first and second side of the rectangular seem. Two sub-plot of this figure are shown in Figure 7 and Figure 8. We can be see from this Figures that for a short period of time at the beginning of this sides of the rectangular seem, ξ_3 is achieved to the needed angle.

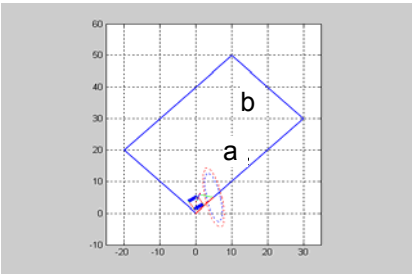

Figure 5: simulated MM for welding of the vessel

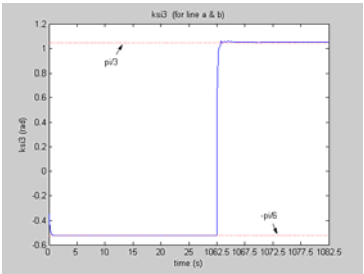

Figure 6: ξ_3 for the beginning of sides(a & b)

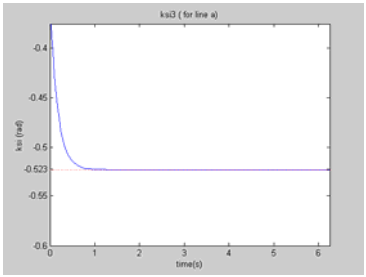

Figure 7: ξ_3 for the beginning of side a.

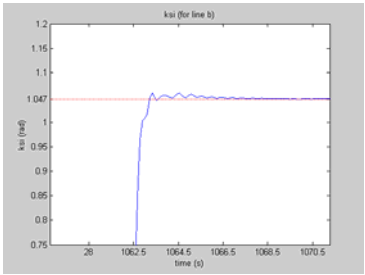

Figure 8: ξ_3 for the beginning of side b.

By optimum design, we observed that for achieved to the desired weld bead shape in this simulation (see Table 2), it is necessary to welding speed of 4 mm/s. Thus, the end effector must be move on seem by this velocity. For this value, the magnitude of $\dot{\xi}_1$ and $\dot{\xi}_2$ is 2.828 mm/s. Figure 9-a shows the magnitude of $\dot{\xi}_1$ for the welding mobile manipulator in the beginning section of first and second side of the rectangular seem. We can be see from this Figure that for the first and second side of seem, $\dot{\xi}_1$ error occurs for a very short time and fit to desired values. Figure 9-b shows the magnitude of $\dot{\xi}_2$ for the welding mobile manipulator in the beginning section of first and second side of the rectangular seem. We can be see from this Figure that for a short period of time at the beginning of the first and second side of the rectangular seem, $\dot{\xi}_2$ is achieved to the needed value of 2.828 mm/s. Finally, Figure 9-c shows the magnitude of welding speed for tracking seem by end effector. the magnitude of welding speed is damped to desired value of 4 mm/s for a very

short time in beginning section of first and second side of the rectangular seem, 15 s for first side and 20 s for second side of seem.

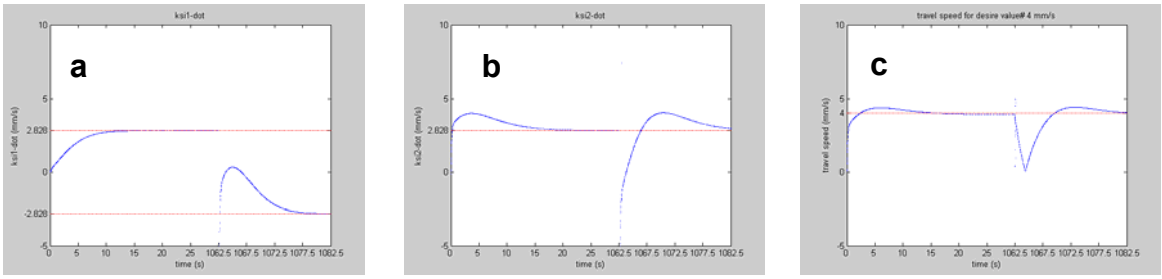

Figure 9:a) $\dot{\xi}_1$ for the beginning of sides(a & b) , b) $\dot{\xi}_2$ for the beginning of sides(a & b) ,c) welding Speed for the beginning of sides(a&b)

8 Conclusion

In this study, a mobile manipulator welding system was designed and analyzed to tracking the weld seem of fillet joint in the vessel, while achieving to the desired weld bead shape was aim of this work. In the first stage of this study, we focused on the geometrical analysis of weldment. Welding process parameters are highly nonlinear characteristics and complex to analyze. Furthermore, the welding process parameters, such as welding speed, Arc voltage, welding current, gas flow rate and offset distance, influencing weld bead shape are coupled with each other. Therefore, there is a limitation to derive the accurate relationship between welding conditions and weld bead shape. To overcome these difficulties, a mathematical method was developed and used to determine the optimal welding conditions for the fillet welded joint shape. and based on the optimum design, the appropriate welding process parameters could be effectively determined.

In the second stage of this study, we used of optimal welding process variables to programming of welding mobile manipulator for tracking the horizontal fillet seem of vessel. From the simulation results, it could be shown that the developed welding mobile manipulator can track the horizontal fillet seam with a fairly good positional accuracy for the optimal fillet welding process parameters, obtained from optimum design.

References

[1] I.S.Kim , W.H.kwon , E.siores ,"An investigation of mathematical model for predicting weld geometry"journal of materials processing technology (1996) pp.385-392.

[2] I.S.Kim, J.S.son ,I.G.kim ,T.Y.kim ,O.S.kim ,"A study on relationship between process variables and bead penetration for robotic CO_2 arc welding " journal of materials processing technology (2003) pp.139-145.

[3] I.S.Kim, J.S.son ,C.E.park ,C.W.lee ,yarlagadda K.D.V.prasad,"A study on prediction of bead heigh in robotic arc welding using a neural network" journal of materials processing technology (2002) pp.229-234.

[4] hyeong –soon moon , suck-joo ,"optimum design based on mathematical model and neural network to predict weld parameters for fillet joints"journal of manufacturing systems .vol.16/No.1 (1997) pp.13-23 .

[5] T . T .Allen , R.W .richardson ,D.P.tagliabue ,G.P.maul ,"statistical process design for robotic GMA welding of sheet metal "welding journal (2002) pp.69-77.

[6] B.bayle, M.renaud ,"nonholonomic mobile manipulators: kinematics ,velocities and redundancies" international conference on robotics and ajournal of intelligent and robotic systems (2003) vol 36 ,pp.45-63.

[7] Bicchi,A. and Prattichizza, D.,2000, ”manipulability of cooperating robots with unactuated joints and closed-chaine mechanisms” IEEE Trans. Robotic Automat.16(4), pp.336 -345.
[8] Park, F.and Kim, J.,1998,”manipulability and singularity analysis of multiple robot systems: A geometric approach” IEEE Trans. Robotic Automat.vo.2, pp.1032 -1037.
[9] Yoshikawa, T.,1985,”manipulability of robotic mechanisms” the international journal of robotics reaserch..vol.2,No.2. pp.3-9.
[10] B.Bayle, J-Y.Forquet , M.Renaud ,” manipulability analysis for Mobile Manipulators”IEEE Trans. Robotic Automat. (2001), pp.1251 -1256.